Neuro-Oncology
22(8), 1190–1202, 2020 | doi:10.1093/neuonc/noaa024 | Advance Access date 6 February 2020

High-grade gliomas in adolescents and young adults highlight histomolecular differences from their adult and pediatric counterparts

Alexandre Roux, Johan Pallud, Raphaël Saffroy, Myriam Edjlali-Goujon, Marie-Anne Debily, Nathalie Boddaert, Marc Sanson, Stéphanie Puget, Steven Knafo, Clovis Adam, Thierry Faillot, Dominique Cazals-Hatem, Emmanuel Mandonnet, Marc Polivka, Georges Dorfmüller, Aurélie Dauta, Mathilde Desplanques, Albane Gareton, Mélanie Pages, Arnault Tauziede-Espariat, Jacques Grill, Franck Bourdeaut, François Doz, Frédéric Dhermain, Karima Mokhtari, Fabrice Chretien, Dominique Figarella-Branger, and Pascale Varlet

Department of Neurosurgery, University Hospital Group (GHU) Paris–Sainte-Anne Hospital, Paris, France (A.R., J.P.); Paris Descartes University, Sorbonne Paris Cité, Paris, France (A.R., J.P., M.E-G., N.B., S.P., A.G., M.P., A.T-E., F.B., F.D., P.V.); Inserm Unit 1266, Imaging Biomarkers of Brain Disorders, Institute of Psychiatry and Neurosciences of Paris, Paris, France (A.R., J.P., M.E-G., M.P., A.T-E., P.V.); Department of Biochemistry, Paul-Brousse Hospital, Villejuif, France (R.S.); Department of Neuroradiology, Sainte-Anne Hospital, Paris, France (M.E-G.); Inserm Unit 981, Biomarkers and New Therapeutic Targets in Oncology Team, Genomics and Oncogenesis of Brain Tumors, Paris-Sud University, Paris-Saclay University, Villejuif, France (M-A. D., J.G.); Evry University, Paris-Saclay University, Evry cedex, France (M-A. D.); Department of Neuroradiology, Necker Enfants-Malades Hospital, Paris, France (N.B., K.M.); Brain and Spine Institute (ICM), Experimental Neuro-Oncology Department, Inserm U1127, Sorbonne University, Paris, France (M.S.); Department of Neurology 2, Mazarin Unit, Pitié-Salpêtrière Hospital, Paris, France (M.S.); Department of Neurosurgery, Necker Enfants-Malades Hospital, Paris, France (S.P.); Department of Neurosurgery, Bicêtre Hospital, Paris-Sud University, Kremlin-Bicêtre, France (S.K.); Department of Pathology, Bicêtre Hospital, Paris-Sud University, Kremlin-Bicêtre, France (C.A.); Department of Neurosurgery, Beaujon Hospital, Clichy, France (T.F.); Department of Pathology, Beaujon Hospital, Clichy, France (D.C-H.); Department of Neurosurgery, Lariboisière Hospital, Paris, France; Paris 7 University, Paris, France (E.M.); Department of Pathology, Lariboisière Hospital, Paris, France (M.P.); Department of Pediatric Neurosurgery, Rothschild Foundation Hospital, Paris, France (G.D.); Department of Neurosurgery, Henri-Mordor Hospital, Créteil, France (A.D.); Department of Pediatric Oncology, Gustave-Roussy University Hospital, Paris-Sud University, Paris-Saclay University, Villejuif, France (J.G.); SIREDO Oncology Center (Care, Innovation and Research for Children and AYA with Cancer), Institut Curie, Paris, France (F.B., F.D.); Department of Radiotherapy, Gustave Roussy University Hospital, Villejuif, France (F.D.); Department of Neuropathology, Pitié-Salpêtrière Hospital, Paris, France (K.M.); Department of Neuropathology, GHU Paris–Sainte-Anne Hospital, Paris, France (M.D.); Department of Pathology and Neuropathology, Timone Hospital, Marseille, France (D.F-B.)

Corresponding Author: Dr Alexandre ROUX, MD, MSc, Service de Neurochirurgie, GHU Paris - Hôpital Sainte-Anne, 1, rue Cabanis, 75674 Paris Cedex 14, France (alexandre.roux@neurochirurgie.fr).

Abstract

Background. Considering that pediatric high-grade gliomas (HGGs) are biologically distinct from their adult counterparts, the objective of this study was to define the landscape of HGGs in adolescents and young adults (AYAs).

Methods. We performed a multicentric retrospective study of 112 AYAs from adult and pediatric Ile-de-France neurosurgical units, treated between 1998 and 2013 to analyze their clinicoradiological and histomolecular profiles. The inclusion criteria were age between 15 and 25 years, histopathological HGG diagnosis, available clinical data, and preoperative and follow-up MRI. MRI and tumoral samples were centrally reviewed. Immunohistochemistry and complementary molecular techniques such as targeted/next-generation sequencing, whole exome sequencing, and DNA-methylation analyses were performed to achieve an integrated diagnosis according to the 2016 World Health Organization (WHO) classification.

Results. Based on 80 documented AYA patients, HGGs constitute heterogeneous clinicopathological and molecular groups, with a predominant representation of pediatric subtypes (histone H3-mutants, 40%) but also adult subtypes (isocitrate dehydrogenase [*IDH*] mutants, 28%) characterized by the rarity of oligodendrogliomas, *IDH* mutants, and 1p/19q codeletion and the relative high frequency of "rare adult *IDH* mutations" (20%). H3G34-mutants (14%) represent the most specific subgroup in AYAs. In the H3K27-mutant subgroup, non-brainstem diffuse midline gliomas are more frequent (66.7%) than diffuse intrinsic pontine gliomas (23.8%), contrary to what is observed in children. We found that WHO grade has no prognostic value, but molecular subgrouping has major prognostic importance.

Conclusions. HGGs in AYAs could benefit from a specific classification, driven by molecular subtyping rather than age group. Collaborative efforts are needed from pediatric and adult neuro-oncology teams to improve the management of HGGs in AYAs.

Key Points

1. Pediatric subtypes (H3G34 and H3K27 mutants) were the most common HGGs in AYAs.
2. Contrary to what is observed in children, non-brainstem diffuse midline gliomas are more frequent than diffuse intrinsic pontine gliomas.
3. WHO grade has no prognostic value contrary to molecular subgrouping.

Importance of the Study

This study highlights that HGG diagnosis in AYAs is often challenging and could benefit from a specialized neuropathological assessment. We found a predominant representation of histone H3 mutants (40%), with non-brainstem diffuse midline gliomas H3K27 mutants (66.7%) and diffuse intrinsic pontine gliomas, H3K27 mutants (23.8%). The H3G34 mutants (14%) had a higher frequency in AYAs than in adult and paediatric population. The *IDH* mutants (28%) were also frequent and characterized by the low rate of oligodendrogliomas and a high frequency of rare *IDH* mutations. This study suggest the major role of the molecular subgrouping to assess new therapeutic strategies in future clinical trial for AYAs.

Primary brain tumors represent the most common solid tumors in children, adolescents and young adults (AYAs).[1] High-grade gliomas (HGGs), according to the World Health Organization [WHO], have the highest mortality rate in patients under the age of 25 years.[2,3] Pediatric HGGs, because of their similar histopathological appearance to adult HGGs, are classified, graded, and treated according to the same system and rationale as adult HGGs. However, recent molecular studies have demonstrated that pediatric HGGs present different genomic alterations and oncogenic activation pathways.[4–7] In addition, comparative genomic hybridization/transcriptome studies have identified different molecular subgroups in adult HGGs,[8] which are rarely found in pediatric HGGs.[9] For instance, isocitrate dehydrogenase 1 and 2 (*IDH1/2*) mutations and 1p/19q codeletion are very rare in children (<3%), as are phosphatase and tensin homolog (PTEN) deletions and epidermal growth factor receptor (EGFR) amplifications (<10%).[10] Contrarily, H3K27M or H3G34R/V variants represent distinct clinicopathological subgroups in pediatrics, and diffuse midline gliomas H3K27M-mutant have even been defined as a new tumoral entity in the WHO 2016 classification of central nervous system tumors.[11] This molecular subgroup is found in 35% of pediatric HGGs with a predominance for diffuse intrinsic pontine gliomas (DIPGs) (36.2%) and non-brainstem diffuse midline gliomas (NB-DMGs) (12.4%)[7] and remains rare in adult HGGs (<3%) and mutually exclusive from *IDH*-mutant cases.[12] There are only scarce available data about HGGs in AYAs,[1] with few studies specifically dedicated to this patient group. Available information can be only extrapolated from pediatric and adult series. Here, we sought to investigate the distribution and clinical, radiological, and histomolecular characteristics of HGGs in AYAs (15–25 year olds), through a retrospective multicentric study with a central histopathological and radiological review to compare them with their adult and pediatric counterparts.

Methods

This retrospective study was conducted in 8 tertiary neurosurgical departments from the Ile-de-France region, France, with pediatric recruitment only (Necker-Enfants Malades), mixed recruitment (Fondation Adolphe de Rothschild), and

adult recruitment only (Sainte-Anne, Lariboisière, Kremlin-Bicêtre, Henri-Mondor, Pitié-Salpêtrière, Beaujon). We used the STROBE (STrengthening the Reporting of OBservational studies in Epidemiology) guidelines to strengthen the methodology.[13] We screened AYA patients treated surgically for a newly diagnosed HGG between January 1998 and December 2013. Inclusion criteria were: (i) patient age between 15 and 25 years at diagnosis; (ii) newly diagnosed HGG, including gliomatosis cerebri, according to the WHO classification in use at the time of surgery; (iii) available histopathological material for central review; and (iv) available clinical records and preoperative MRI.

A flow chart detailing the inclusion process is presented in Figure 1.

Clinical Data Assessment

Clinical data were obtained from medical records by 2 neurosurgeons (A.R. and J.P.) while blind to imaging, histopathological, molecular data, and outcomes. Clinical data included: sex, age, Karnofsky performance status (KPS), past medical history, physical examination at diagnosis, first-line oncological treatment, oncological treatments at progression, progression-free survival (PFS), and overall survival (OS). PFS was measured from the date of histopathological diagnosis to the date of evidence of progression or to the date of death. Tumor progression was defined according to the Macdonald criteria in use at the time of management by any of the following: (i) 25% increase in total perpendicular diameters of an enhancing lesion, (ii) any new lesion, or (iii) clinical deterioration. OS was measured from the date of histopathological diagnosis to the date of death from any cause. Surviving patients were censored at the date of last follow-up.

Imaging Assessment

We performed a centralized review of all pre- and postoperative MRIs by a senior pediatric neuroradiologist (N.B.)

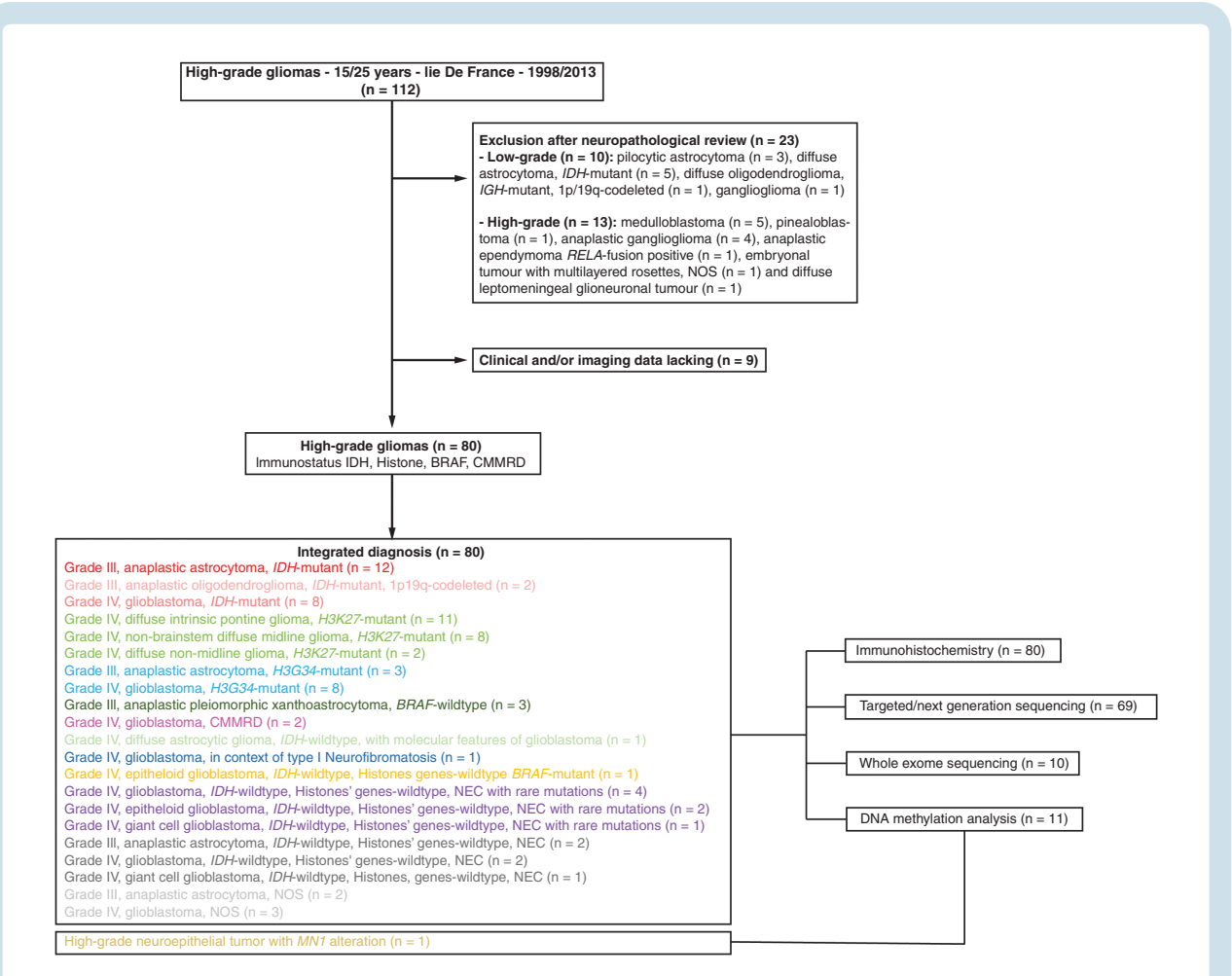

Fig. 1 Patient flow chart. According to our inclusion criteria, 112 AYA patients were initially included in this study. After central neuropathological review, we excluded 23 patients with no HGGs: 10 for low-grade tumors and 13 for high-grade tumors. We excluded 9 patients for clinical and/or imaging data lacking. Finally, 80 AYA patients were included in this study and we proposed an integrated diagnosis for all of them. Eighty patients had immunohistochemistry, 69 targeted/next-generation sequencing, 10 WES, and 11 DNA-methylation analysis.

and a senior adult neuroradiologist (M.E-G.) while blind to clinical, histopathological, molecular data, and outcomes. Imaging was performed at the time of the diagnosis using either a 1.5 Tesla or a 3 Tesla MRI scanner, depending on the institution. Image data included: main topography, side, leptomeningeal involvement, ependymal contact, and contrast enhancement. The extent of resection was quantified based on early postoperative (within 48 h) MRI.

Neuropathological Review

A centralized neuropathological review consisted of an independent reassessment by 3 senior neuropathologists (P.V., K.M., and D.F.B.), members of the RENOCLIP-LOC network (REseau National de Neuro-Oncologie CLInico-Pathologique—Lymphomes Oculo-Cérébraux, France [National Network of Clinicopathological Neuro-Oncology—Oculo-Cerebral Lymphomas]) while blind to clinical, imaging, molecular data, and outcomes. The objective was to confirm the initial diagnosis of HGG according to the WHO 2016 classification using additional immunostainings (Ki-67, GFAP, Olig2, IDH1-R132H, ATRX, p53, H3K27M, H3K27me3, G34R, BRAFV600E, NF70, CD34, MLH1, MSH2, MSH6, PMS2) if necessary. The 3 reviewers completed an identical evaluation form. In case of discrepancy, the final diagnosis was reached by consensus. All details of our methodology for immunohistochemistry, sequencing techniques, whole-exome sequencing (WES), and DNA-methylation analysis are available in the Supplementary data.

Integrated Diagnosis Analysis

Integrated diagnoses were performed after central histopathological and radiological reviews and after obtaining the molecular data, by one experienced neuropathologist (P.V.). Midline involvement and the main tumor location were important data to collect in order to refine our molecular subgroups (ie, NB-DMG, H3K27-mutant). Tumor contrast enhancement and leptomeningeal spread were also reported. If classical immunophenotypical and/or molecular characteristics such as *IDH1/2*, histone, or *BRAF* mutations were found by targeted/next-generation sequencing, subsequent analyses were stopped. If not, complementary molecular techniques were pursued (WES and/or DNA-methylation analysis), depending on tumor/blood availability.

Literature Analysis

A literature search was conducted via the US National Library of Medicine (PubMed/MEDLINE) to collect recent available data on pediatric and adult HGGs (from January 2010 to December 2018). "High-grade glioma," "glioblastoma," and "anaplastic astrocytoma" were used as specific search terms. All retrieved titles and abstracts were screened. All full-text publications were reviewed for each potentially eligible study. The references of the articles were reviewed to supplement the initial search. Publications were eligible if they were: (i) full-text articles written in English and (ii) cohort studies with publicly available data. For each case, data of interest were entered into a dedicated form designed for the study.

Online Repository

The whole raw anonymous clinical, imaging, histopathological, and molecular data were registered on the French glioblastoma biobank (https://nantes-lrsy.hugo-online.fr/CSOnline/Accueil.aspx). At the end of the data collection, processed data were exported from this site for statistical analyses.

Statistical Analysis

All statistical analyses were realized based on WHO 2016 integrated diagnosis. Univariate analyses were carried out using chi-square or Fisher's exact test for comparing categorical variables, and the unpaired *t*-test or Mann–Whitney rank-sum test for continuous variables, as appropriate. The Kaplan–Meier method, using log-rank tests to assess significance for group comparisons, plotted unadjusted survival curves for PFS and OS. A Cox proportional hazards model was performed in a multivariate analysis. We created Cox proportional hazards regression models on the whole series using a backward stepwise approach, adjusting for predictors previously associated at the $P < 0.2$ level with mortality and recurrence in unadjusted analysis. A probability value <0.05 was considered statistically significant. Statistical analyses were performed using JMP software v14.1.0 (SAS Institute).

Ethics Statement

This study has been declared to the French National Agency for Medicines and Health Products Safety (ANSM, ID-RCB 2015-A00206–43) and received the required authorizations of the National Data Information and Freedom Commission (CNIL, DR-2016–227, n91616) and the French Ethics Committee of Protection of Persons (CPP, 2015-A00206–43, DCF3349). Patients consented to the extraction of data from their medical records.

Results

Clinical and Imaging Characteristics

A total of 112 AYA patients were screened (Figure 1). Main patient characteristics are detailed in Supplementary Table 1. The cohort included 80 patients with a median age at diagnosis of 21 years (range, 15–25). Hemispheric supratentorial location was predominant (68.7%), midline involvement was found in 18.8%, and bilateral involvement was found in 12.5%. Concerning first-line treatment, surgical resection was performed in 70% of cases and a radiotherapy and/or chemotherapy protocol was followed in 93.8% of cases, which closely resembles adult neuro-oncological management. We found a significant association between midline location and age <18 years at diagnosis ($P = 0.019$).

Immunohistochemical and Molecular Techniques

As illustrated in Supplementary Figure 1, all HGG samples benefited from immunohistochemistry analyses.

Complementary molecular analyses could not be performed in 11 cases (13.7%) due to lack of material. Targeted/next-generation sequencing was done in 69 cases (86.3%). Therefore, integrated diagnoses could be established in 60 cases (75%) with routine techniques. When enough material was available, WES and DNA-methylation analyses were subsequently performed if previous techniques did not allow for a precise tumor classification. WES (n = 10) confirmed 2 diagnoses and refined 8 HGG diagnoses. DNA-methylation analysis (n = 11) established a new diagnosis of high-grade neuroepithelial tumor with meningioma 1 gene (*MN1*) alteration (high-grade neuroepithelial tumor [HGNET], *MN1*; score: 0.45) in 1 case, refined one diagnosis (glioblastoma, RTKII; score 0.88), and was non-informative in 9 cases.

Integrated Diagnosis

The integrated clinical, imaging, histopathological, and molecular characteristics are detailed in Figure 2. We found significant differences between the age at diagnosis and the HGG molecular subgroups (P = 0.014), with a significant higher frequency of patients younger than 18 years affected with H3K27-mutant, H3G34-mutant, and pleomorphic xanthoastrocytoma 3 (PXAIII) subgroups, contrary to *IDH*-mutant, epithelioid and giant cell glioblastoma, and other glioma subgroups.

The most common molecular subgroup consisted of "pediatric-type" histones' genes-mutants (n = 32, 40.0%). We found 21 H3K27-mutants (26.3%) distributed according to the location in: NB-DMG (n = 14), DIPG (n = 5), and diffuse non-midline glioma (n = 2). Within the molecularly defined H3K27-mutants (n = 19/21, 90.5%), we found 1 H3.1 variant (5.3%) in a DIPG and 18 H3.3 variants (94.7%). One of H3K27-mutants (DIPG, grade IV, H3K27-mutant) was a rare variant (H3K27I) (4.8%).

Eleven H3G34-mutants (13.7%) were graded as anaplastic astrocytoma, grade III (n = 3), or glioblastoma, grade IV (n = 8). All of the H3G34-mutants were G34R-mutants (100%) and all of them had a hemispheric supratentorial location, while 19 H3K27-mutants (90.5%) involved the midline, with a significant difference (P < 0.001). The median ages at diagnosis were 18 years (range, 15–21) and 20 years (range, 15–25) for H3G34-mutants and H3K27-mutants, respectively. Concerning the H3K27-mutant subgroup, age at diagnosis was statistically different (P = 0.046) according to the main tumor location: 16 years (range, 15–20) for DIPG, 21 years (range, 15–25) for NB-DMG, and 22 years (range, 21–23) for diffuse non-midline glioma.

The second molecular subgroup consisted of "adult-type" *IDH*-mutants (n = 22, 27.5%), including 20 astrocytomas, *IDH*-mutant (25%) (anaplastic astrocytoma, grade III, *IDH*-mutant [n = 12], and glioblastoma, grade IV, *IDH*-mutant [n = 8]) and 2 oligodendrogliomas, grade III, *IDH*-mutant and 1p/19q codeleted (2.5%). Five *IDH*-mutants were "rare adult" variants (2 *IDH1-R132G*, 1 *IDH1-R132C*, 1 *IDH1-R132S*, and 1 *IDH2-R172W*) (22.7%). All *IDH*-mutants had a hemispheric supratentorial location and the median age at diagnosis was 22.5 years (range, 18–25). Concerning

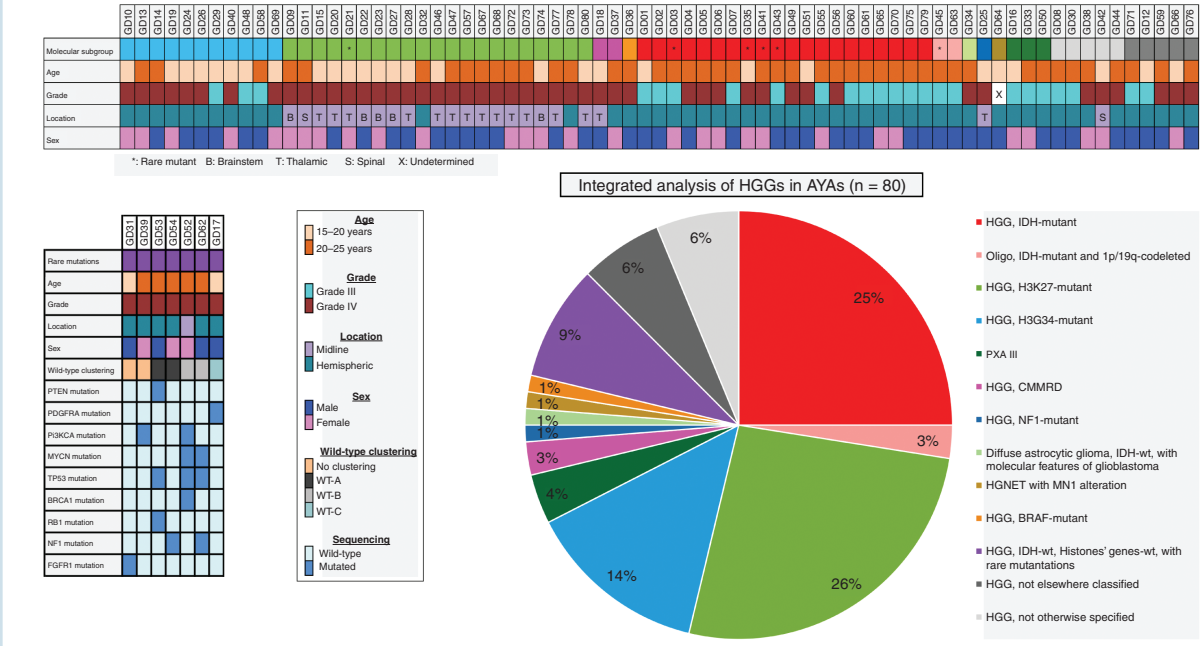

Fig. 2 Integrated analysis description (n = 80). Oncoprint chart representing our integrated analysis according to the molecular subgroups. We describe age, histopathological grading, anatomical location, and sex. For AYA patients with rare mutations (down and left) we add results of the next-generation sequencing. We propose a pie chart of our integrated analysis describing the frequency of histo-radio-molecular subgroups.

the *IDH*-mutant subgroups, for astrocytomas, grades III/IV, *IDH*-mutant, and oligodendrogliomas, grade III, *IDH*-mutant and 1p/19q codeleted, the median ages at diagnosis were 23 years (range, 18–25) and 20.5 years (range, 19–22), respectively.

We found 3 PXAIII, *BRAF*-wildtype (3.8%) with a median age at diagnosis of 25 years (range, 16–25) and a hemispheric location, 2 glioblastomas grade IV, constitutional mismatch repair deficiency (2.5%) (16 and 20 y) with a hemispheric location, 1 diffuse astrocytic glioma, grade IV, *IDH*-wildtype, with molecular features of glioblastoma (1.3%) (21 y), and a hemispheric location, 1 glioblastoma, grade IV, in the context of type I neurofibromatosis (1.3%) (19 y) with a midline location, and 1 epithelioid glioblastoma, grade IV, *BRAF*-mutant (1.3%) (24 y) with a hemispheric location.

Then, WES (n = 10) allowed us to specify the molecular characteristics of 6 cases of grades III/IV HGG not elsewhere classified (NEC) with rare mutations (7.5%). The median age was 21 years (range, 15–25). *NF1*, *TP53*, *Pi3KCA*, *MYCN*, and *PTEN* were the most frequent rare mutants found in AYAs (Fig. 2). In line with Mackay et al,[7] we classified these cases in 3 subgroups: (i) WT-A, which corresponded to HGG driven by *BRAFV600E*, *NF1* mutations, or fusions in receptor tyrosine kinases including *MET*, *FGFR2*, and *NTRK2/3*; (ii) WT-B, which corresponded to HGG associated with chromosome 2 gains, amplifications in *EGFR*, *CDK6*, and *MYCN*; and (iii) WT-C, which corresponded to HGG associated with chromosome 1p and 20q loss and 17q gain and harbored *PDGFRA* and *MET* amplifications. Five tumors were distributed into WT-A (n = 2), WT-B (n = 2), or WT-C (n = 1) HGGs, according to their molecular alteration profiles, but 2 remained as not classified.

Finally, DNA-methylation analysis (n = 11) found 9 cases with no match (81.8%), 1 glioblastoma *IDH*-wildtype, 1 GBM RTKII (9.1%), and 1 case of non-HGG with a diagnosis of HGNET-*MN1* (9.1%). Thus, the neuropathological review confirmed the diagnosis of HGG in 98.8% of cases. Diagnosis changed following extensive genomic and epigenomic profiling in one case (1.2%) of non-HGG, which was an HGNET-*MN1*.

Neuroradiological Analysis of Molecularly Defined HGGs

The 14 NB-DMG, H3K27-mutant patients (17.5%) presented a tumoral contrast enhancement (78.6%) with (85.7%) or without (14.3%) necrosis. Concerning the 5 DIPGs (6.3%), they involved the pons but also the midbrain in 80% of cases and leptomeningeal compartment in 20% of cases. The 2 diffuse non-midline gliomas (2.5%) involved the parietal lobe and presented with contrast enhancement and necrosis. H3G34-mutants involved mainly the parietal (45.5%) and the frontal (36.4%) lobes. All of them presented with contrast enhancement, and necrosis was found in 72.7% of cases. Leptomeningeal spread was found in 9.1% of cases.

IDH-mutants involved only the frontal (72.8%) and the temporal (18.2%) lobes. Contrast enhancement was found in 68.2% of cases and in all glioblastoma cases with (22.7%) or without (77.3%) necrosis. Calcifications were found in only one case (4.5%), which was an oligodendroglioma.

Literature Analysis

We have collected publicly available data from 23 recent pediatric and adult HGG cohorts with molecular data.[4,9,12,14–33] We were careful to subtract 321 AYA cases from this review in order to elucidate the distribution of molecular subgroups in this particular age group (15–25 y) and to compare them with purely pediatric (<15 y) and adult (>25 y) cases. Otherwise, we collected recent publicly available data from the largest pediatric[7] and 2 adult cohort[34,35] studies comprising globally 2646 cases: pediatric (<15 y, n = 1012), adolescent (15–25 y, n = 321), and adult (26–55 y, n = 1313). We compared the distribution of AYA molecular subgroups from their adult (26–55 y) and strictly pediatric (<15 y) counterparts. The comparative molecular subgroup distribution in the 3 age groups is illustrated in Figure 3.

Survival Analysis

A simplified graphical summary illustrating the different subgroups of HGGs identified by the present integrated classification is given in Figure 5.

During follow-up (mean, 34.7 mo; range, 0.1–147.1 mo), 73 patients (91.3%) experienced tumor progression, which was histopathologically proven in 18 cases (22.5%) following a second surgical resection, and 67 patients (83.8%) died from tumor progression. Kaplan–Meier curves are detailed in Figure 4A. The median PFS was 13.9 months (95% CI: 12.0–21.0) and the median OS was 25.4 months (95% CI: 18.8–28.8). The details of the survival results for each molecular subgroup are shown in Figure 4B–G.

Prognostic Factor Analyses

Unadjusted and adjusted risk factors of OS are detailed in Table 1. A significant association with OS in univariate analyses was found with the following: epilepsy at diagnosis (unadjusted hazard ratio [uHR], 0.45 [95% CI: 0.26–0.79], P = 0.003), increased intracranial pressure at diagnosis (uHR, 2.08 [95% CI: 1.19–3.62], P = 0.007), altered KPS at diagnosis (uHR, 9.40 [95% CI: 2.75–32.16], P = 0.006), midline location (uHR, 2.16 [95% CI: 1.25–3.72], P = 0.008), Ki-67 index >50% (uHR, 6.63 [95% CI: 2.20–19.96], P = 0.003), whole integrated molecular classification (uHR, 4.90 [95% CI: 2.28–10.53], P < 0.001), histopathological grade IV (uHR, 1.74 [95% CI: 1.00–3.02], P = 0.041), surgical resection (uHR, 0.49 [95% CI: 0.29–0.82], P = 0.009), and subtotal and total resection (uHR, 0.44 [95% CI: 0.24–0.79], P = 0.025). After adjustments using multivariate Cox models, the following each had an independent association with OS: older age at diagnosis (adjusted hazard ratio [aHR], 0.30 [95% CI: 0.11–0.80], P = 0.017), altered KPS at diagnosis (aHR, 12.63 [95% CI: 3.10–51.42], P = 0.004), whole integrated molecular classification (aHR, 10.02 [95% CI: 2.47–40.67], P = 0.040), and subtotal and total resection (aHR, 0.37 [95% CI: 0.18–0.80], P = 0.043).

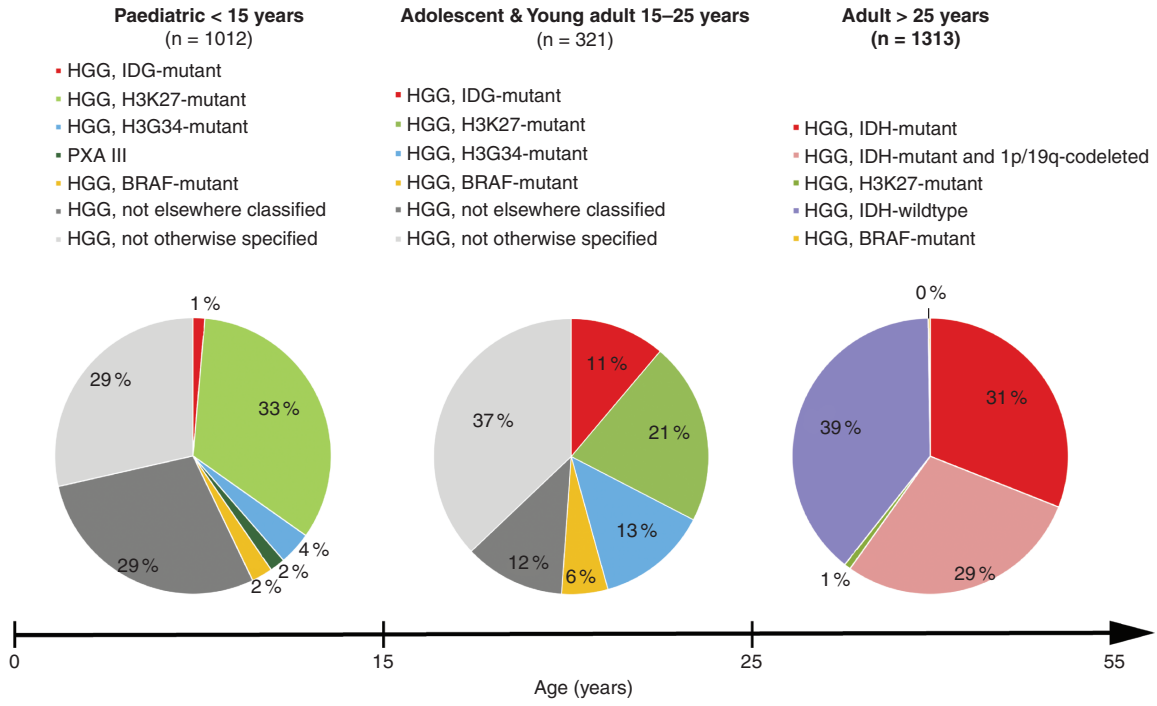

Fig. 3 Comparative analysis of published HGG cases by molecular and age subgroups. After literature review, we realized 3 pie charts describing the distribution of histo-radio-molecular subgroups for HGGs by age group: (i) pediatric (<15 y), (ii) adolescent and young adult (15–25 y), and (iii) adult (25–55 y). We could appreciate the different distribution of these histo-radio-molecular subgroups according to the age.

Discussion

This is the first study to assess the clinical, imaging, histopathological, and molecular landscape of HGGs in the AYA population. Neuropathological review led to the rejection of 20.5% of cases, including 9 cases (8%) reclassified as low-grade gliomas. In our study, the percentage of neuropathological rejection (20.5%) was higher than in the HERBY trial (12.3%), which could be due to the difficulty of analyzing HGGs in AYAs when neuropathologists analyze samples from adult recruitment only. In our study, the rejection rate is 6.2% in centers with mixed recruitment versus 14.3% in centers with adult and AYA recruitment only.

After extensive molecular analyses, all but one case diagnosed by the central neuropathological review were confirmed. An HGNET-*MN1* was diagnosed based on WES and confirmed by DNA-methylation analysis. This reinforces the notion that morphological aspects and new immunophenotyping tools with specific antibodies and sequencing techniques are sufficient to permit an adequate histomolecular diagnosis (72.5% of cases). WES and DNA-methylation analysis could be useful only in a minority of particularly complex cases.

In our study, the most common molecular subgroup consisted of "pediatric-type" histones' genes-mutants (40.0%), and H3G34-mutant HGGs (14%) remain the most specific molecular subgroup (Fig. 2). As previously described, H3G34-mutants have a higher frequency in AYAs (13%) than in pediatric (4%) and adult (<1%) populations (Fig. 3). The typical aspect is of a supratentorial contrast-enhancing tumor involving the parietal and/or occipital lobes in an AYA patient[36] (Fig. 5).

H3K27-mutants represent a frequent molecular subgroup in AYAs (Fig. 2), which is characterized by frequent midline involvement, with partial surgical resection or biopsy,[37] and by a resistance to radiotherapy and chemotherapy protocols.[38] H3K27-mutants in AYAs (21%) are more common than in their adult counterpart (1%), but rarer than in the pediatric population (33%) (Fig. 3). Otherwise, in the 80 patients included in this study, we found a lower rate of midline tumors (18.8%) compared with the HERBY trial (35%), and a decreasing frequency with age in AYA patients, which could be due to a pediatric specificity of H3K27-mutants. The lower frequency of H3.1 variants (17%)[7] could be explained by a more frequent non-brainstem location (66.7%) than pontine location (23.8%) in H3K27-mutant AYA patients compared with pediatric patients (29.6% and 68.3%, respectively) (Fig. 2 and 5). There was no imaging specificity of H3K27-mutants in AYAs compared with children,[39] except midbrain involvement and the leptomeningeal spread. We found a higher rate of midbrain involvement in AYA cases (80%) than in a previous report based on children (55.2%).[40] We found a decreasing frequency of DIPG H3K27-mutants

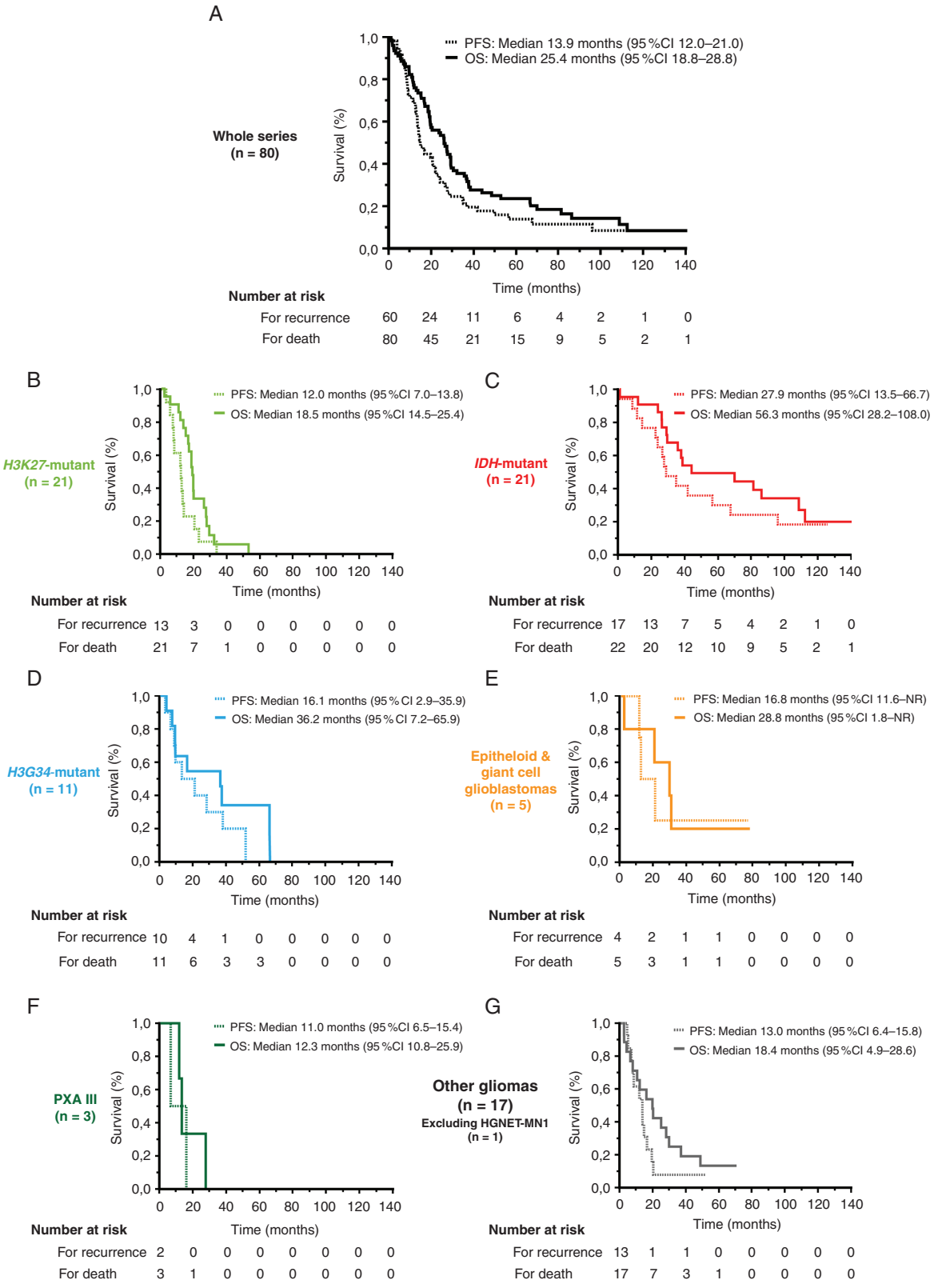

Fig. 4 Kaplan–Meier curves describing PFS (dashed lines) and OS (continuous lines) in (A) the whole series, (B) the H3K27-mutants, (C) the IDH-mutants, (D) the H3G34-mutants, (E) the epithelioid and giant cell glioblastomas, (F) the anaplastic pleomorphic xantroastrocytomas, and (G) the other gliomas (excluding the HGNET-*MN1* case).

Table 1 Univariate and multivariate analyses of factors associated with overall survival ($N = 79$)

Parameters	*n*	Univariate Analysis			Multivariate Analysis		
		Unadjusted Hazard Ratio	95% CI	*P*-value	Adjusted Hazard Ratio	95% CI	*P*-value
Clinical characteristics							
Sex							
Male	48 / 79	1.16	0.71–1.90	0.554			
Female	31 / 79	1					
Older age at diagnosis (per unit, year)	79 / 79	0.54	0.25–1.17	0.118	0.30	0.11–0.80	**0.017**
Epilepsy at diagnosis							
No	54 / 79	1					
Yes	25 / 79	0.45	0.26–0.79	**0.003**			
Neurological deficit at diagnosis							
No	41 / 79	1					
Yes	38 / 79	1.54	0.95–2.51	0.083			
Increased intracranial pressure at diagnosis							
No	24 / 79	1			1		
Yes	55 / 79	2.08	1.19–3.62	**0.007**	1.80	0.96–3.38	0.060
Karnofsky performance status at diagnosis							
< 70	3 / 79	9.40	2.75–32.16	**0.006**	12.63	3.10–51.42	**0.004**
≥ 70	76 / 79	1			1		
Imaging characteristics							
Midline location							
No	56 / 79	1			1		
Yes	23 / 79	2.16	1.25–3.72	**0.008**	0.60	0.23–1.57	0.307
Leptomeningeal spread							
No	73 / 79	1					
Yes	6 / 79	2.15	0.92–5.03	0.109			
Contrast enhancement							
No	11 / 79	1					
Yes	68 / 79	2.02	0.93–4.38	0.056			
Histopathological characteristics							
Integrated molecular classification							
HGG, IDH-mutant	22 / 79	1			1		
HGG, H3K27-mutant	21 / 79	4.90	2.28–10.53	**<0.001**	2.58	0.67–10.03	**0.040**
HGG, H3G34-mutant	11 / 79	2.37	0.99–5.70		1.04	0.34–3.17	
Anaplastic pleomorphic xanthoastrocytoma	3 / 79	6.97	1.87–25.93		10.02	2.47–40.67	
Epithelioid and giant cells glioblastoma	5 / 79	2.26	0.73–7.05		2.03	0.59–7.00	
Other gliomas	18 / 79	3.79	1.75–8.22		3.62	1.49–8.82	
Histopathological grade							
III	23 / 79	1			1		
IV	56 / 79	1.74	1.00–3.02	**0.041**	1.13	0.54–2.36	0.738
Mitoses for 10 high power fields							

Table 1 Continued

Parameters	*n*	Univariate Analysis			Multivariate Analysis		
		Unadjusted Hazard Ratio	95% CI	*P*-value	Adjusted Hazard Ratio	95% CI	*P*-value
<5	35 / 79	1					
5–10	24 / 79	0.84	0.46–1.54	0.531			
>10	20 / 79	1.23	0.69–2.18				
Ki-67 index							
<5%	9 / 79	1			1		
5–20%	43 / 79	2.39	0.98–5.79	**0.003**	2.16		
21–50%	19 / 79	3.79	1.45–9.87		3.79		
>50%	8 / 79	6.63	2.20–19.96		6.18		
Treatment-related characteristics							
Surgical treatment							
Biopsy	24 / 79	1					
Resection	55 / 79	0.49	0.29–0.82	**0.009**			
Extent of resection							
Biopsy	24 / 79	1			1		
Partial resection	25 / 79	0.56	0.30–1.02	**0.025**	0.47	0.20–1.10	**0.043**
Subtotal and total resection	30 / 79	0.44	0.24–0.79		0.37	0.18–0.80	
First-line adjuvant oncological treatment							
None	5 / 79	1					
Chemotherapy only	2 / 79	0.40	0.04–3.61	0.251			
Radiotherapy only	17 / 79	0.73	0.24–2.24				
Radiotherapy + adjuvant chemotherapy	9 / 79	1.78	0.53–5.97				
Combined radiochemotherapy + adjuvant chemotherapy	46 / 79	1.14	0.40–3.24				

with age but an increasing frequency of NB-DMG H3K27-mutants in AYAs before becoming rare in adults. Moreover, we found 2 diffuse non-midline gliomas, H3K27-mutants (*n* = 2/21, 9.5%), which were confirmed by sequencing and imaging reassessment. This rare entity has previously been described, involving the temporal, frontal, or parietal lobes,[12,32] but not specifically in the AYA population.[12,32]

"Adult-type" *IDH*-mutants were the second most frequent molecular subgroup (11%) in the literature, with an intermediate prevalence between pediatric (1%) and young adult (60%) populations (Fig. 3). However, the higher rate of *IDH*-mutant HGGs (28%) in our study compared with the literature (11%) (Fig. 2 and 3) could be explained by the majority of adult neurosurgical centers in our recruitment process. Interestingly, we found a high rate of "rare" adult variants in the *IDH*-mutant subgroup (*n* = 5/22, 22.7%; two *IDH1R132G*, one *IDH1R132C*, one *IDH1R132S*, and one *IDH2R172W*), with a distinct distribution from what was reported by a previous report based on AYA HGGs.[10] The *IDH*-mutant subgroup in our AYA study is characterized by the low rate of oligodendrogliomas *IDH* mutant and 1p/19q codeleted (one *IDH1-R132H* and one *IDH2-R172W*) (3%) (Fig. 2) compared with their adult counterpart (29%).[33–35] Oligodendrogliomas *IDH* mutant and 1p/19q codeleted are found even more rarely in the pediatric population.[41] Finally, imaging characteristics of *IDH*-mutant HGGs in AYAs were similar to the adult population, especially the frontal and temporal lobe predominance.[42]

We found only one case of *BRAF*-mutant HGG (epithelioid glioblastoma, grade IV [1.3%]), which was lower than in the literature (6%) (Fig. 3). This result could be explained in part by the exclusion of 3 cases considered as gangliogliomas, grade III, *BRAF*-mutant, during the neuropathological review.

Mackay et al recently suggested a classification of *IDH*-wildtype and histones' genes-wildtype pediatric HGG subgroups into 3 distinct molecular subgroups (WT-A, WT-B, and WT-C) with particular genetic alterations.[7] Here, we identified 5 cases corresponding to WT-A (*n* = 2), WT-B (*n* = 2), and WT-C (*n* = 1) but 2 remained as not classified (Fi. 2).

Otherwise, we found various types of HGGs after the integrated analysis (Fig. 2 and 5), which suggests a molecular heterogeneity in AYA and justifies the need for molecular assessment in routine clinical practice for this specific population. Finally, we found a lower rate of

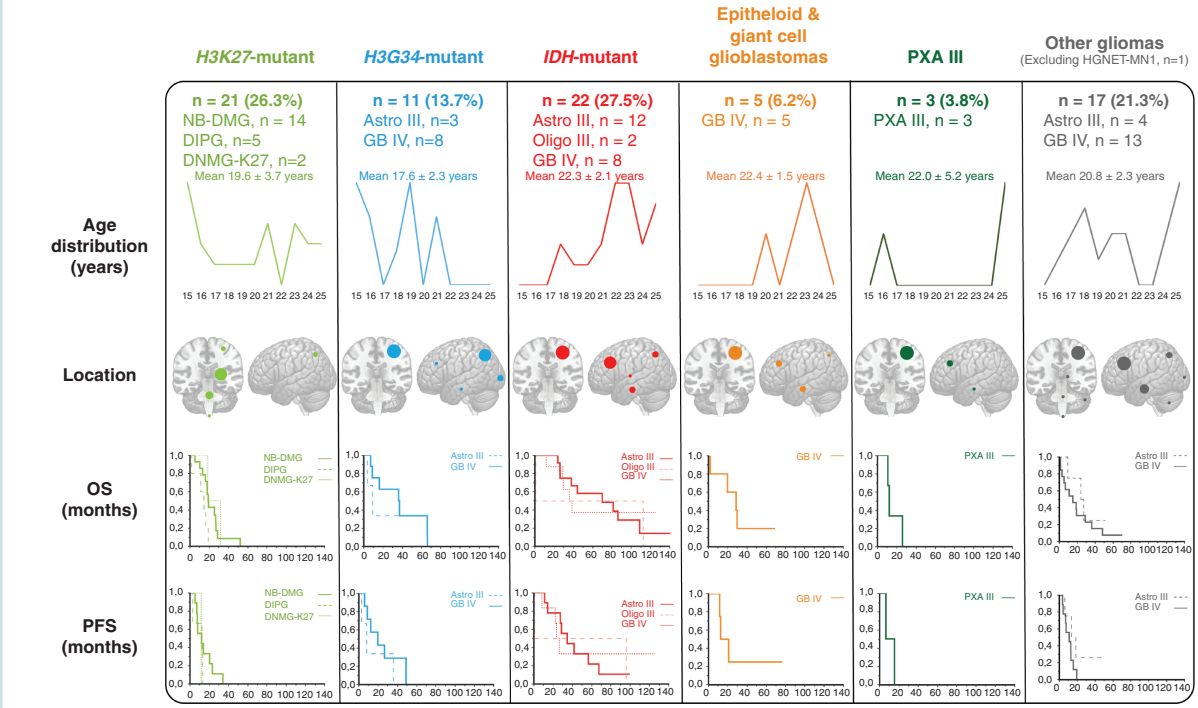

Fig. 5 Graphical summary of integrated molecular subgroups in adolescents and young adults ($n = 79$). Simplified schematic representation of key clinical, radiological, and survival results in 6 high-grade glioma subgroups according to our integrated histo-radio-molecular analysis.

HGGs NOS (not otherwise specified) in our study and an almost similar rate of HGGs NEC (6% and 15%, respectively) compared with the current literature concerning AYAs (37% and 12%, respectively) thanks to imaging reassessments and immunohistochemical, targeted/next-generation sequencing, and advanced molecular techniques (Figu. 2 and 3).

Interpretation

The results should be interpreted with full knowledge of the retrospective design of the study. However, we found no prognostic value for grade III versus IV using the updated WHO 2016 classification guidelines. This is consistent with the results from the randomized HERBY study dedicated to pediatric HGGs[43] but also with large adult HGG cohorts.[34,35] This also reinforces the fact that the prognostic value of each key grading criteria should be established in each different molecular HGG entity. Furthermore, prognostic significance of tumor grading in the context of a non-molecularly defined HGG is possible, but underlines the importance of integrated molecular classification. The Ki-67 index was identified as a factor impacting survival in our study, which is consistent with a previous report focusing on pediatric HGGs.[43]

However, we found a significant impact of the extent of surgical resection on OS in univariate and multivariate analyses, as previously described in pediatric[44] and adult[45] populations harboring an HGG.

In multivariate analyses, we found a significant independent impact of the integrated molecular classification for HGG in AYAs ($P = 0.040$), which highlights the importance of molecularly driven classification of these tumors. These findings suggest that in protocol designs, treatment allocation according to age should be mitigated by molecular diagnosis through the close collaboration between adult and pediatric neuro-oncology teams.

We observed that *IDH*-mutant HGGs, which remain a rare entity in the pediatric population, occurred more frequently in patients older than 20 years and were only involved in hemispheric supratentorial tumors with a higher prevalence in the frontal lobe (Fig. 5). This observation argues for similar management of *IDH*-mutant HGGs in the AYA population and of HGGs in adults. NB-DMG had a better prognosis than DIPGs, with a median OS of 19.1 months compared with 14.5 months, respectively. This difference could be explained by the location of the tumor, but also by the accessibility of surgical resection for midline tumors.[37] We acknowledge a decreasing prevalence of H3K27-mutants[32] and an increasing prevalence of *IDH*-mutants with age,[4,25] but H3G34-mutants, which were rarely found in pediatric and adult patients, appear to be a specific subgroup of AYAs (Fig. 5). Due to the rarity of histones' genes-mutant HGGs in adults, the management of these tumors in AYAs could be aligned with new pediatric oncological treatments.[38,46]

Conclusion

HGGs in AYAs are heterogeneous clinicopathological and molecular subgroups of tumors, with a predominant representation of the pediatric subtype (H3K27-mutants, 40%) and a higher proportion of non-brainstem H3K27-mutants, but also some adult subtypes (*IDH*-mutants, 27.5%) with 2 characteristics: (i) the rarity of oligodendrogliomas *IDH*-mutant and 1p/19q codeleted, and (ii) the relative high frequency of the so-called "rare adult *IDH* mutations" (20%). H3G34-mutants were found to be the AYA-specific molecular subgroup, with a higher frequency than in pediatric and adult patients. Interestingly, we found that WHO grade III versus IV has no prognostic value in this cohort, but molecular subgrouping has major prognostic importance. Our study suggests the importance to assess HGGs in AYAs by molecular subgroup rather than age group. Collaborative efforts are needed between pediatric and adult neuro-oncology teams to move forward in the care management of HGGs in AYAs.

Supplementary Material

Supplementary data are available at *Neuro-Oncology* online.

Keywords

DNA-methylation analysis | glioblastoma | glioma | integrated diagnosis | whole exome sequencing

Funding

This study was supported by the Ligue Contre le Cancer (PRADO2014.LNCC/PV).

Acknowledgments

The authors would like to thank the Ligue Nationale Contre le Cancer for their financial support. The authors gratefully acknowledge (in alphabetical order): the French glioblastoma biobank; the Integragen platform; and the RENOCLIP-LOC, supported by the Institut National du Cancer (INCa). Alexandre Roux would like to thank the Nuovo-Soldati Foundation for Cancer Research for their support.

Conflict of interest statement. The authors declare that they have no conflict of interest.

Authorship statement. *Data collection*: AR, JP, RS, MEG, MAD, NB, MS, SP, SK, CA, TF, DCH, EM, GD, AD, MD, ATE, JG, FB, FD, FD, KM, DFB, PV. *Data analysis*: AR, JP, RS, MEG, MAD, NB, MS, SP, SK, CA, TF, DCH, EM, MP, GD, AD, MD, AG, MP, ATE, JG, FB, FD, FD, KM, FC, DFB, PV. *Data interpretation*: AR, JP, RS, MEG, MAD, NB, MS, SP, SK, CA, TF, DCH, EM, MP, GD, AD, MD, AG, MP, ATE, JG, FB, FD, FD, KM, FC, DFB, PV. *Report writing*: AR, JP, RS, MEG, MAD, NB, MS, SP, SK, CA, TF, DCH, EM, MP, GD, AD, MD, AG, MP, ATE, JG, FB, FD, FD, KM, FC, DFB, PV. *Proofreading and paper approval*: AR, JP, RS, MEG, MAD, NB, MS, SP, SK, CA, TF, DCH, EM, MP, GD, AD, MD, AG, MP, ATE, JG, FB, FD, FD, KM, FC, DFB, PV.

References

1. Diwanji TP, Engelman A, Snider JW, Mohindra P. Epidemiology, diagnosis, and optimal management of glioma in adolescents and young adults. *Adolesc Health Med Ther.* 2017;8:99–113.
2. Leibetseder A, Ackerl M, Flechl B, et al. Outcome and molecular characteristics of adolescent and young adult patients with newly diagnosed primary glioblastoma: a study of the Society of Austrian Neurooncology (SANO). *Neuro Oncol.* 2013;15(1):112–121.
3. Ostrom QT, Gittleman H, Truitt G, Boscia A, Kruchko C, Barnholtz-Sloan JS. CBTRUS statistical report: primary brain and other central nervous system tumors diagnosed in the United States in 2011-2015. *Neuro Oncol.* 2018;20(suppl_4):iv1–iv86.
4. Paugh BS, Qu C, Jones C, et al. Integrated molecular genetic profiling of pediatric high-grade gliomas reveals key differences with the adult disease. *J Clin Oncol.* 2010;28(18):3061–3068.
5. Qu HQ, Jacob K, Fatet S, et al. Genome-wide profiling using single-nucleotide polymorphism arrays identifies novel chromosomal imbalances in pediatric glioblastomas. *Neuro Oncol.* 2010;12(2):153–163.
6. Sturm D, Bender S, Jones DT, et al. Paediatric and adult glioblastoma: multiform (epi)genomic culprits emerge. *Nat Rev Cancer.* 2014;14(2):92–107.
7. Mackay A, Burford A, Carvalho D, et al. Integrated molecular meta-analysis of 1,000 pediatric high-grade and diffuse intrinsic pontine glioma. *Cancer Cell.* 2017;32(4):520–537.e5.
8. Brennan CW, Verhaak RG, McKenna A, et al; TCGA Research Network. The somatic genomic landscape of glioblastoma. *Cell.* 2013;155(2):462–477.
9. Wu G, Diaz AK, Paugh BS, et al. The genomic landscape of diffuse intrinsic pontine glioma and pediatric non-brainstem high-grade glioma. *Nat Genet.* 2014;46(5):444–450.
10. Pollack IF, Hamilton RL, Sobol RW, et al; Children's Oncology Group. IDH1 mutations are common in malignant gliomas arising in adolescents: a report from the Children's Oncology Group. *Childs Nerv Syst.* 2011;27(1):87–94.
11. Louis DN, Perry A, Reifenberger G, et al. The 2016 World Health Organization classification of tumors of the central nervous system: a summary. *Acta Neuropathol. (Berl.)* 2016;131(6):803–820.
12. Sturm D, Witt H, Hovestadt V, et al. Hotspot mutations in H3F3A and IDH1 define distinct epigenetic and biological subgroups of glioblastoma. *Cancer Cell.* 2012;22(4):425–437.
13. von Elm E, Altman DG, Egger M, Pocock SJ, Gøtzsche PC, Vandenbroucke JP; STROBE Initiative. The Strengthening the

Reporting of Observational Studies in Epidemiology (STROBE) statement: guidelines for reporting observational studies. *Lancet.* 2007;370(9596):1453–1457.
14. Arita H, Yamasaki K, Matsushita Y, et al. A combination of TERT promoter mutation and MGMT methylation status predicts clinically relevant subgroups of newly diagnosed glioblastomas. *Acta Neuropathol Commun.* 2016;4(1):79.
15. Barrow J, Adamowicz-Brice M, Cartmill M, et al. Homozygous loss of ADAM3A revealed by genome-wide analysis of pediatric high-grade glioma and diffuse intrinsic pontine gliomas. *Neuro Oncol.* 2011;13(2):212–222.
16. Bender S, Tang Y, Lindroth AM, et al. Reduced H3K27me3 and DNA hypomethylation are major drivers of gene expression in K27M mutant pediatric high-grade gliomas. *Cancer Cell.* 2013;24(5):660–672.
17. Carvalho D, Mackay A, Bjerke L, et al. The prognostic role of intragenic copy number breakpoints and identification of novel fusion genes in paediatric high grade glioma. *Acta Neuropathol Commun.* 2014;2:23.
18. Castel D, Philippe C, Calmon R, et al. Histone H3F3A and HIST1H3B K27M mutations define two subgroups of diffuse intrinsic pontine gliomas with different prognosis and phenotypes. *Acta Neuropathol.* 2015;130(6):815–827.
19. Fontebasso AM, Papillon-Cavanagh S, Schwartzentruber J, et al. Recurrent somatic mutations in ACVR1 in pediatric midline high-grade astrocytoma. *Nat Genet.* 2014;46(5):462–466.
20. Fontebasso AM, Schwartzentruber J, Khuong-Quang DA, et al. Mutations in SETD2 and genes affecting histone H3K36 methylation target hemispheric high-grade gliomas. *Acta Neuropathol.* 2013;125(5):659–669.
21. Gessi M, Gielen GH, Dreschmann V, Waha A, Pietsch T. High frequency of H3F3A (K27M) mutations characterizes pediatric and adult high-grade gliomas of the spinal cord. *Acta Neuropathol.* 2015;130(3):435–437.
22. Herrlinger U, Jones DTW, Glas M, et al. Gliomatosis cerebri: no evidence for a separate brain tumor entity. *Acta Neuropathol.* 2016;131(2):309–319.
23. International Cancer Genome Consortium PedBrain Tumor Project. Recurrent MET fusion genes represent a drug target in pediatric glioblastoma. *Nat Med.* 2016;22(11):1314–1320.
24. Kline CN, Joseph NM, Grenert JP, et al. Targeted next-generation sequencing of pediatric neuro-oncology patients improves diagnosis, identifies pathogenic germline mutations, and directs targeted therapy. *Neuro Oncol.* 2017;19(5):699–709.
25. Korshunov A, Ryzhova M, Hovestadt V, et al. Integrated analysis of pediatric glioblastoma reveals a subset of biologically favorable tumors with associated molecular prognostic markers. *Acta Neuropathol.* 2015;129(5):669–678.
26. Korshunov A, Chavez L, Northcott PA, et al. DNA-methylation profiling discloses significant advantages over NanoString method for molecular classification of medulloblastoma. *Acta Neuropathol.* 2017;134(6):965–967.
27. Lohkamp LN, Schinz M, Gehlhaar C, et al. MGMT promoter methylation and BRAF V600E mutations are helpful markers to discriminate pleomorphic xanthoastrocytoma from giant cell glioblastoma. *PLoS One.* 2016;11(6):e0156422.
28. Paugh BS, Broniscer A, Qu C, et al. Genome-wide analyses identify recurrent amplifications of receptor tyrosine kinases and cell-cycle regulatory genes in diffuse intrinsic pontine glioma. *J Clin Oncol.* 2011;29(30):3999–4006.
29. Porkholm M, Raunio A, Vainionpää R, et al. Molecular alterations in pediatric brainstem gliomas. *Pediatr Blood Cancer.* 2018;65(1). doi: 10.1002/pbc.26751.
30. Puget S, Philippe C, Bax DA, et al. Mesenchymal transition and PDGFRA amplification/mutation are key distinct oncogenic events in pediatric diffuse intrinsic pontine gliomas. *PLoS One.* 2012;7(2):e30313.
31. Salloum R, McConechy MK, Mikael LG, et al. Characterizing temporal genomic heterogeneity in pediatric high-grade gliomas. *Acta Neuropathol Commun.* 2017;5(1):78.
32. Schwartzentruber J, Korshunov A, Liu XY, et al. Driver mutations in histone H3.3 and chromatin remodelling genes in paediatric glioblastoma. *Nature.* 2012;482(7384):226–231.
33. Zhang RQ, Shi Z, Chen H, et al. Biomarker-based prognostic stratification of young adult glioblastoma. *Oncotarget.* 2016;7(4):5030–5041.
34. Tabouret E, Nguyen AT, Dehais C, et al; for POLA Network. Prognostic impact of the 2016 WHO classification of diffuse gliomas in the French POLA cohort. *Acta Neuropathol.* 2016;132(4):625–634.
35. Pekmezci M, Rice T, Molinaro AM, et al. Adult infiltrating gliomas with WHO 2016 integrated diagnosis: additional prognostic roles of ATRX and TERT. *Acta Neuropathol (Berl).* 2017;133(6):1001–1016.
36. Puntonet J, Dangouloff-Ros V, Saffroy R, et al. Historadiological correlations in high-grade glioma with the histone 3.3 G34R mutation. *J Neuroradiol.* 2018;45(5):316–322.
37. Cinalli G, Aguirre DT, Mirone G, et al. Surgical treatment of thalamic tumors in children. *J Neurosurg Pediatr.* 2018;21(3):247–257.
38. Cohen KJ, Jabado N, Grill J. Diffuse intrinsic pontine gliomas—current management and new biologic insights. Is there a glimmer of hope? *Neuro Oncol.* 2017;19(8):1025–1034.
39. Aboian MS, Solomon DA, Felton E, et al. Imaging characteristics of pediatric diffuse midline gliomas with histone H3 K27M mutation. *AJNR Am J Neuroradiol.* 2017;38(4):795–800.
40. Roux A, Boddaert N, Grill J, et al. High prevalence of developmental venous anomaly in diffuse intrinsic pontine gliomas: a pediatric control study. *Neurosurgery.* 2019. doi: 10.1093/neuros/nyz298.
41. Nauen D, Haley L, Lin MT, et al. Molecular analysis of pediatric oligodendrogliomas highlights genetic differences with adult counterparts and other pediatric gliomas. *Brain Pathol.* 2016;26(2):206–214.
42. Wang Y, Zhang T, Li S, et al. Anatomical localization of isocitrate dehydrogenase 1 mutation: a voxel-based radiographic study of 146 low-grade gliomas. *Eur J Neurol.* 2015;22(2):348–354.
43. Varlet P, Le Teuff G, Le Deley M-C, et al. WHO grade has no prognostic value in the pediatric high-grade glioma included in the HERBY trial. *Neuro Oncol.* 2019. doi: 10.1093/neuonc/noz142.
44. MacDonald TJ, Aguilera D, Kramm CM. Treatment of high-grade glioma in children and adolescents. *Neuro Oncol.* 2011;13(10):1049–1058.
45. Roux A, Roca P, Edjlali M, et al. MRI atlas of IDH wild-type supratentorial glioblastoma: probabilistic maps of phenotype, management, and outcomes. *Radiology.* 2019. doi: 10.1148/radiol.2019190491.
46. Grill J, Massimino M, Bouffet E, et al. Phase II, Open-label, randomized, multicenter trial (HERBY) of bevacizumab in pediatric patients with newly diagnosed high-grade glioma. *J Clin Oncol.* 2018;36(10):951–958.